Environmental Earth Sciences (2020) 79:25
https://doi.org/10.1007/s12665-019-8749-3

ORIGINAL ARTICLE

Effects of shape, inlet blockage and wing walls on local scour at the outlet of non-submerged culverts: undermining of the embankment

Álvaro Galán[1] · Javier González[1]

Received: 2 November 2018 / Accepted: 27 November 2019

Abstract
Drainage works using culverts are potentially affected by local scour risk. Local scour process is a complex phenomenon affected by many factors. Most of them have been analyzed in previous studies, either individually or in small groups. However, no fully joint analysis has been developed so far. Since the number of factors and interactions is high, the main objective of this work was to determine which of them best represents the dimensions of the scour hole and the embankment undermining. 80 experiments have been designed and developed and studied by ANOVA techniques. These results highlight the effect of wing walls with a floor slab at the outlet and the inlet blockage, showing them to be of major importance. The influence of the tailwater depth and the culvert shape on the scour hole are confirmed as relevant factors, as well as the presence of wing walls. Some interactions have been identified as relevant. The main outcome of this work is the set of factors and interactions that has significant impact on local scour process occurring beside a culvert. This selection is the basis for performing further experimental work in the future to obtain a general empirical law that quantifies this kind of local scour.

Keywords Culvert local scour · Embankment undermining · Culvert wing walls · Hydrology risk · Non-submerged culverts

Introduction

Transportation networks are of major importance for the transport of people and goods and, therefore, for the economy of a country, and as such they can be considered as critical infrastructures (Heimbecher and Kaundinya 2010). These networks affect the natural surface drainage pattern of watersheds and produce an unnatural concentration of water run-off at drainage structures, mainly culverts. As a consequence, the modification of the flow yields to an excess of kinetic energy at the culvert outlet that makes culverts a potential source of local scour (Opie 1967). Besides, due to the large number of existent culverts, small and medium-size ones are often constructed without measures to prevent scour (Day et al. 2001) which can lead to an excessive undermining of the culvert structure, causing failure of the structure and the embankment (Abt et al. 1996; Mendoza et al. 1983).

Several studies have been performed with the aim of understanding the complex scour phenomenon at flat jet, 2D and 3D jets outlets (circular and square shapes mainly) during the past decades [see Breusers and Raudkivi (1991) for further details of the different types of jet]. Some authors like Chen (1970) or Abt et al. (1987) concluded that, under the same flow rate, a square culvert with a height equal to the diameter, d, of a circular one, would reduce the maximum scour depth, $d_{s,max}$, defined as the vertical distance from the original (flat) bed elevation to the deepest point in the longitudinal scour profile. In contrast, some other works, e.g., Bohan (1970), pointed out that with low tailwater depths, i.e., $Y_t \lesssim 0.5d$, the culvert shape has little or no influence on the scour hole geometry. Some of early experimental works for circular culverts are those by Ruff et al. (1982), Mendoza et al. (1983) or Abt et al. (1984). For squared culverts there are fewer works but to mention some, the reader is referred to those by Abida and Townsend (1991), Karki et al. (2007) or Sorourian (2015).

✉ Álvaro Galán
alvaro.galan@uclm.es

Javier González
javier.gonzalez@uclm.es

[1] E.T.S.I. Caminos, Canales y Puertos (UCLM), Avda. Camilo José Cela s/n, 13071 Ciudad Real, Spain

Published online: 17 December 2019

As noted above, Y_t is one important factor which influences local scour and therefore it has been broadly approached for both emerged ($Y_t/d \leq 1$) and submerged jets ($Y_t/d \geq 1$). A complete record of some experiments with non submerged jets carried out by other authors can be found in Day et al. (2001). One of the highlights is that a critical value of Y_t/d exists for which a maximum value of scour depth is yielded. This critical value has been found to be close to $Y_t/d \approx 0.5$ (Bohan 1970). For very low tailwater depths, i.e., $Y_t/d < 0.2$, the formation of a high mound over which the flow can not discharge material leads to a decrease of $d_{s,max}$, as pointed out by Abida and Townsend (1991). More recently, Emami and Schleiss (2006) revealed that for very low tailwater depths $d_{s,max}$ decreases but the scour hole develops closer to the pipe outlet, which could produce the undermining of the embankment and its collapse. To the author's knowledge, no studies to analyze the undermining of the embankment have been conducted to date, even though this phenomenon is, perhaps, the most important one when analysing the embankment stability.

All previously mentioned works were carried out with an uniform non-cohesive sediment, so that the maximum scour depth is not expected to be diminished by armouring effect (Abida and Townsend 1991), as happens when the granulometric dispersion $\sigma_g \equiv \sqrt{d_{84}/d_{16}} \geq 1.3$. Abt et al. (1984) is perhaps the first work that explicitly includes σ_g into the predictive equations for the scour hole geometry. For non-cohesive uniform sediments, the mean sediment size, d_{50}, has been shown to be an important parameter to properly predict the scour hole dimensions. According to Abida and Townsend (1991), although the hole width, W_s, which represents the extent of lateral expansion of the scour hole is independent of d_{50}, the greater the d_{50} the smaller the maximum scour depth within the hole, $d_{s,max}$. However, it has been widely assumed (Ali and Lim 1986; Day et al. 2001; Sarathi et al. 2008) that the effect of the sediment size on scour hole dimensions is mostly absorbed by the densimetric Froude number, F_0, defined as

$$F_0 = \frac{U_0}{\sqrt{g\Delta d_{50}}}, \tag{1}$$

where U_0 is the mean flow velocity just at the culvert outlet, g is the gravitational acceleration and $\Delta \equiv (\rho_s - \rho)/\rho$ is the relative submerged density of the sediment where ρ_s and ρ are the sediment and fluid density respectively. The densimetric Froude number, which represents the ratio of the tractive force on a sediment particle to the submerged specific weight of the sediment (Day et al. 2001), has been clearly imposed upon some other characteristic parameters like the Froude number at the outlet, the intensity discharge parameter introduced by Ruff et al. (1982) or its modified version defined by Donnell and Abt (1983). The influence of F_0 on the scour hole dimensions seems to be clear in values of up to $F_0 \approx 10$, where $d_{s,max}$ increases with F_0 (Lim 1995). Additionally, Sorourian et al. (2014a, b) and Sorourian (2015) recently reported an increment of 22% in maximum scour depth and up to 25% for the scour hole width when a culvert is partially blocked at the inlet, and that the location of maximum scour depth occurs closer to the culvert outlet with respect to the condition of non-blocked culverts. This is due to the fact that the resultant turbulent flow both throughout the barrel and at the outlet are quite different for partially blocked and non-blocked conditions with the same discharge.

Apart from $d_{s,max}$, the location of maximum scour depth, $L_{s,max}$, defined as the horizontal distance measured along the longitudinal centreline between the culvert outlet and the point where $d_{s,max}$ takes place, is also important since if the maximum scour depth occurs near the embankment, it is easier for embankment failure to arise. From previous studies it can be concluded that $L_{s,max}$ varies between $0.25L_s$ (Fletcher and Grace 1972) and $0.7L_s$ (Lim 1995), where L_s is the scour hole length, defined as the longitudinal distance from the culvert outlet to the downstream limit of scour. However, the location of maximum scour depth could be larger as tailwater depth, Y_t, increases (Kells et al. 2001) or smaller for culverts with headwall at the outlet (Mendoza et al. 1983). Even though these elements at the inlet/outlet of culverts are very usual, very few studies have dealt with their effects on the scour at the outlet. For instance, Abida and Townsend (1991) noted that with high flow rates wing walls are not able to promote an efficient redistribution of velocity across the downstream channel section, and so it can yield to failure by undermining the culvert floor slab. In that work, they also noted that the restriction on lateral expansion of the outlet jet imposed by the receiving downstream channel width, B, has to be considered as an accurate prediction of scour. It is generally assumed that the expansion ratio, defined as B/d, has no influence for values $B/d \gtrsim 10$ (Lim 1995). For values below that limit, B/d does not have influence either if both F_0 and Y_t are sufficiently large (Sui et al. 2008).

Within this context, several predictive equations based mainly on experimental measurements for scour hole geometry in both unsteady (instantaneous scour) and asymptotic (equilibrium scour) conditions have been presented. Melville and Lim (2014) compiled most of the previous data and formulations for local scour depth with 2D horizontal jets to develop a new and unified prediction equation. Other researchers have employed other techniques like Neural Networks (Liriano and Day 2001), Gene-Expression Programming (Azamathulla and Haque 2012) or CFD (Boroomand et al. 2007; Karim and Ali 2000) to correctly estimate scour at culvert outlets with quite good results. However, data related to the undermining of the structure, the effects of

wing walls at the outlet or the partial blockage at the inlet are still scarce. Additionally, as noted by Day et al. (2001), most of the published data on culvert scour has been collected from relatively small-scale physical models.

Given the above background and the underexplored effect of wing walls, which are frequently used in real applications, the present study intends to analyze the effect of a wing walled outlet with a floor slab and blockage at the inlet on the local scour with two culvert geometries (mainly the maximum scour depth, $d_{s,max}$ and its location, $L_{s,max}$). This study also aims to understand the influence of some variables on the undermining of the associated embankment. Hence a cantilevered embankment above the granular channel is employed.

A set of 80 experiments over square and circular shaped culverts ($d = 0.153$ m) with non submerged outlets ($Y_t/d \leq 1$) has been carried out for this purpose. The objective is to understand and identify those factors which have a greater effect in the associated undermining. The effects will be classified by an ANOVA analyses, which will result in a qualitative factor influence classification. The results will be the main reference for performing deeper, more detailed experimental work on the selected factor in the future, to obtain experimental equations on which to model associated undermining characteristics.

As for temporal evolution, local scour at culvert outlets is a temporal phenomenon with different phases that occur during the process (scour beginning, digging, filling, re-occurrence of digging) which have been studied by, among others, Kells et al. (2001), Karki et al. (2007) and Balachandar and Reddy (2013) for different flow conditions, tailwater depths ranges and culvert shapes. There has been no consensus on the equilibrium time, understood as the required time for the scour hole to reach a stable condition. For instance, Mendoza et al. (1983) concluded that the 95% of scour is reached during the first 500 min, while Ade and Rajaratman (1998) stated that the equilibrium time is even greater that 8 days. It seems clear, however, that the equilibrium time increases as F_0 increases (Rajaratnam and Berry 1977) and that the closer is the outlet, the smaller the time to reach the asymptotic state (Faruque et al. 2006). Since we are interested in the factors affecting the embankment undermining (i.e., scour close to the culvert outlet) we will not consider the time as a main variable in the experiments if we ensure a reasonable duration of them.

Framework for analysis

Figure 1 shows a scheme of the case under consideration. As can be observed from the 3D view, fluid goes into the transparent culvert through an initial reservoir supplied by pumps. Two video cameras are located at the dry zone limited by two vertical walls that simulate the embankment. The receiving channel is composed by sediment (brown color) at the first 4 m and a bed made of concrete where the gate is installed to fix the tailwater depth. Note that sediment bed extends below the rigid embankment in order to allow the undermining of the structure.

For a non-cohesive sediment (the most unfavourable of the cases), horizontal barrels and null offset vertical distance, we can write for any dimension of scour hole (assuming equilibrium state)

$$\xi = \psi\left(\rho, \nu, g, d_{50}, \sigma_g, \rho_s, B, d, Y_u, Y_t, Q, L, k_s\right), \tag{2}$$

where ξ is any scour hole dimension, ψ is an unknown function to be obtained, ν is the kinematic viscosity of fluid, Y_u is the headwater depth, Q is the flow rate and L and k_s are the culvert length and roughness, respectively (the rest of the variables have already been presented throughout the introduction).

Note that above, the flow rate can be related with other variables

$$Q = \psi\left(\rho, \nu, g, d, Y_u, Y_t, L, k_s\right),$$

and one of them should be eliminated from the analysis. However, since we want to consider the inlet blockage and the outlet configuration in the problem, we cannot eliminate Q from Eq. 2. By dimensional analysis we can write

$$\frac{\xi}{d} = \psi\left(\frac{\nu^2}{gd^3}, \frac{d_{50}}{d}, \sigma_g, \Delta, \frac{B}{d}, \frac{Y_u}{d}, \frac{Y_t}{d}, \frac{Q^2}{gd^5}, \frac{L}{d}, \frac{k_s}{d}\right). \tag{3}$$

Some factors have to be taken into consideration in order to simplify Eq. 3:

1. viscous effects and roughness of barrel are negligible. According to Day et al. (2001) scale effects are negligible when the pipe Reynolds number is $Re \geq 5 \times 10^4$.
2. the submerged relative density of sediment, Δ, can be considered constant (≈ 1.65) and only influencing on the submerged weight
3. the channel bed material is composed of uniform ($\sigma_g \leq 1.3$) non-ripple forming sand ($d_{50} > 0.60$ mm)
4. the effect of mean sediment size, d_{50}, is properly absorbed if F_0 is employed
5. the effects of the channel walls are negligible, which implies $B/d \geq 10$
6. the length of the culvert related to its rise takes usual values in practice, i.e., $L/d \approx 10-15$. This value has been obtained by analysing more than 200 culverts in road transport networks in the province of Ciudad Real (Spain) where $L/d = 10.6 \pm 6.1$.

Under the considerations outlined above, Eq. 3 reads

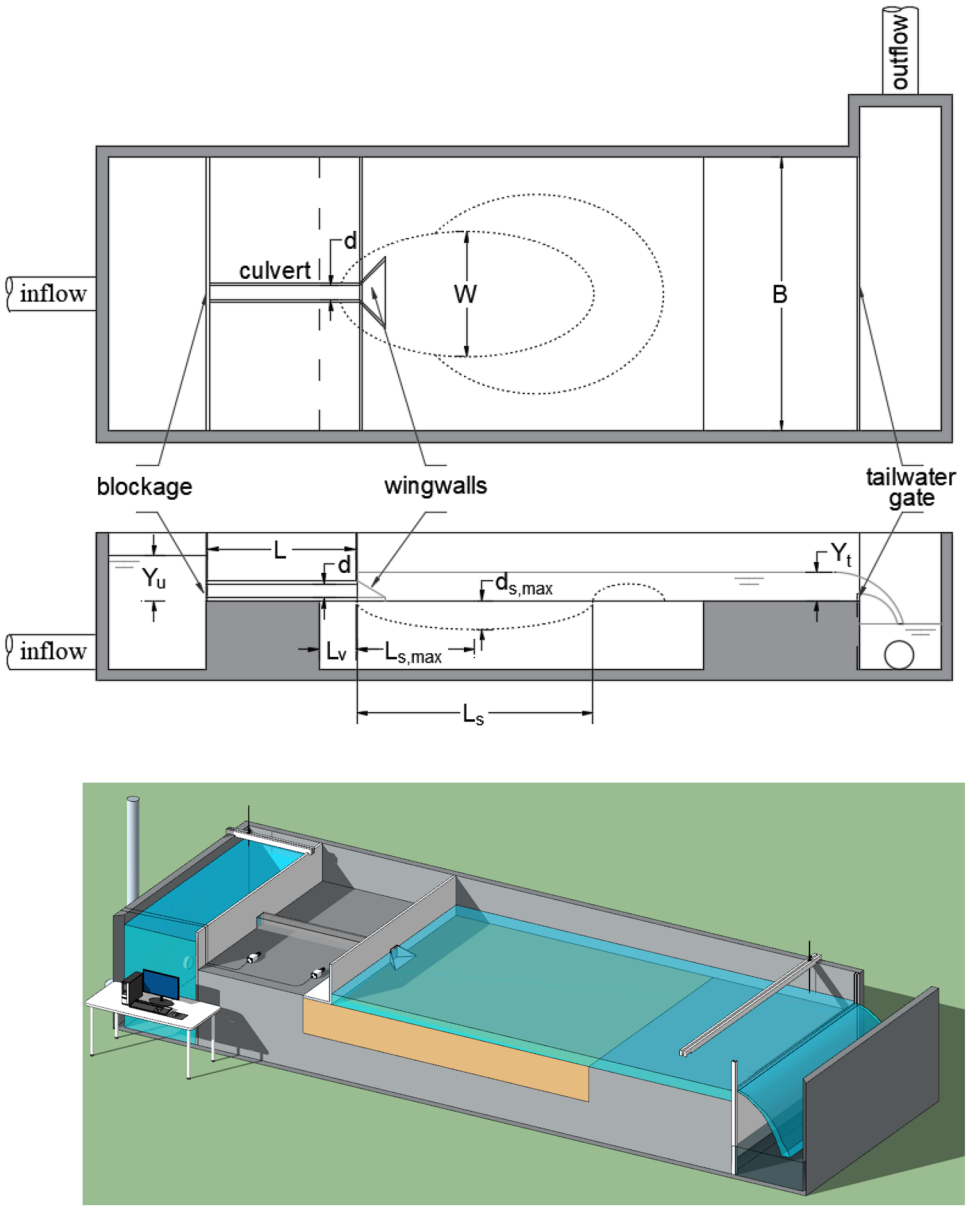

Fig. 1 Schematic approach to the problem with the main lengths in plant view (top), profile view (middle) and 3D view (bottom)

$$\frac{\xi}{d} = \psi\left(\frac{Y_u}{d}, \frac{Y_t}{d}, F_0\right), \tag{4}$$

which is the base for the experimental campaign. Note that function ψ will be different for any combination of culvert shape, culvert outlet configuration and blockage at the inlet.

Experiments

The experiments were carried out in a 4 m-long and 3 m-wide (area covered with a 0.7 m-thick sediment) horizontal flume at the Civil Engineering School Hydraulics Laboratory (University of Castilla-La Mancha, Spain). The sediment was a quartzitic sediment with density $\rho_s \approx 2650$ kg/m^3, median size $d_{50} = 1.20$ mm and granulometric dispersion $\sigma_g \approx 1.2 < 1.3$ [i.e., uniform sediment according to Abt et al. (1984)], so armouring effects could be neglected and the maximum scour depth was expected. Barrels of circular and square shapes made of methacrylate were employed with the same values of $d = 0.153$ m and $L = 2.0$ m for both shapes ($L/d \approx 13$). With these values, the expansion ratio, $B/d \approx 19.6 \geq 10$, ensured that the channel width had no influence on the scour hole geometry. As shown in Fig. 1, a cantilevered configuration for the simulated embankment, made of PVC, above the sediment bed was used to allow the undermining of the structure if needed. By employing this configuration, the degree of undermining that the culvert produces on the embankment in different experiments could be measured. For instance, Fig. 2 shows a photograph

of the final state of the experiment *C004* in Table 1 and the embankment undermining characterized by the transversal area scoured at the outlet section behind the rigid embankment, A_u.

For each combination of input culvert blockage (0% for non-blocked culverts and 50% for partially blocked culverts) and outlet configuration (with and without wing walls with a floor slab), ten

Table 1 Control variables of the tests, flow rate and densimetric Froude number at the culvert outlet

Circular shape ○							Square shape □						
Test	Y_u/d	Y_t/d	Q (l/s)	Y_0 (m)	U_0 (m/s)	F_0	Test	Y_u/d	Y_t/d	Q (l/s)	Y_0 (m)	U_0 (m/s)	F_0
Without wing walls at outlet and non-blocked inlet (0% blockage)													
C000	0.50	0.12	6.63	0.054	1.140	8.2	S000	0.46	0.15	6.75	0.039	1.120	8.0
C001	1.23	0.16	11.48	0.103	0.875	6.3	S001	1.25	0.26	14.11	0.060	1.534	11.0
C002	1.23	0.63	11.56	0.116	0.775	5.6	S002	1.26	0.64	13.96	0.083	1.105	7.9
C003	1.25	1.00	11.04	0.153	0.600	4.3	S003	1.23	1.00	11.99	0.153	0.512	3.7
C004	1.87	0.23	16.04	0.153	1.111	8.0	S004	2.05	0.34	28.95	0.091	2.084	15.0
C005	1.99	0.65	17.49	0.121	1.118	8.0	S005	1.95	0.59	27.74	0.121	1.505	10.8
C006	1.99	1.03	18.93	0.153	1.030	7.4	S006	1.97	1.13	24.77	0.153	1.058	7.6
C007	2.21	0.25	19.10	0.115	1.292	9.3	S007	2.45	0.35	32.75	0.092	2.332	16.7
C008	2.35	0.64	18.66	0.107	1.363	9.8	S008	2.50	0.62	27.20	0.074	2.409	17.3
C009	2.44	1.06	22.93	0.153	1.247	8.9	S009	2.36	1.04	29.51	0.153	1.261	9.0
With wing walls at outlet and non-blocked inlet (0% blockage)													
C010	0.53	0.15	6.59	0.064	0.910	6.5	S010	0.58	0.13	7.88	0.049	1.043	7.5
C011	1.21	0.14	11.44	0.108	0.822	5.9	S011	1.26	0.21	13.60	0.096	0.930	6.7
C012	1.22	0.60	11.19	0.112	0.777	5.6	S012	1.25	0.62	13.77	0.098	0.919	6.6
C013	1.26	1.00	11.03	0.153	0.600	4.3	S013	1.24	0.98	12.73	0.153	0.544	3.9
C014	1.97	0.19	17.21	0.114	1.174	8.4	S014	1.89	0.25	25.53	0.102	1.630	11.7
C015	1.94	0.59	17.51	0.116	1.167	8.4	S015	1.96	0.59	28.03	0.153	1.197	8.6
C016	1.87	1.04	17.79	0.153	0.968	6.9	S016	1.98	1.06	25.53	0.153	1.091	7.8
C017	2.46	0.22	20.97	0.100	1.649	11.8	S017	2.52	0.26	28.08	0.101	1.814	13.0
C018	2.38	0.63	20.30	0.110	1.433	10.3	S018	2.44	0.59	32.66	0.153	1.395	10.0
C019	2.42	1.05	23.06	0.153	1.254	9.0	S019	2.38	1.04	29.51	0.153	1.261	9.0
Without wing walls at outlet and partially blocked inlet (50% blockage)													
C100	0.52	0.12	5.12	0.050	0.975	7.0	S100	0.55	0.16	6.38	0.034	1.237	8.9
C101	1.25	0.16	9.81	0.096	0.807	5.8	S101	1.24	0.17	10.76	0.066	1.062	7.6
C102	1.27	0.61	9.80	0.107	0.717	5.1	S102	1.28	0.59	10.46	0.090	0.762	5.5
C103	1.27	0.97	9.26	0.153	0.504	3.6	S103	1.27	0.98	9.94	0.153	0.425	3.0
C104	2.02	0.20	12.07	0.090	1.070	7.7	S104	1.97	0.20	12.43	0.069	1.179	8.5
C105	2.01	0.65	11.36	0.087	1.060	7.6	S105	1.97	0.64	12.41	0.084	0.969	7.0
C106	1.87	1.02	11.42	0.153	0.621	4.5	S106	1.97	1.02	13.52	0.153	0.578	4.1
C107	2.51	0.21	12.07	0.087	1.121	8.0	S107	2.47	0.22	15.43	0.071	1.426	10.2
C108	2.23	0.64	11.36	0.083	1.124	8.1	S108	2.48	0.66	15.21	0.071	1.402	10.1
C109	2.46	1.02	13.17	0.153	0.716	5.1	S109	2.45	1.05	17.32	0.153	0.740	5.3
With wing walls at outlet and partially blocked inlet (50% blockage)													
C110	0.43	0.10	4.42	0.043	1.040	7.5	S110	0.55	0.18	6.27	0.033	1.242	8.9
C111	1.25	0.18	9.73	0.088	0.888	6.4	S111	1.29	0.16	10.89	0.077	0.924	6.6
C112	1.28	0.63	10.00	0.095	0.833	6.0	S112	1.23	0.61	10.67	0.087	0.797	5.7
C113	1.26	0.96	9.17	0.153	0.499	3.6	S113	1.30	0.95	10.34	0.153	0.442	3.2
C114	2.06	0.18	11.42	0.083	1.114	8.0	S114	1.74	0.13	11.98	0.075	1.047	7.5
C115	2.04	0.63	11.48	0.100	0.904	6.5	S115	2.03	0.59	12.70	0.083	0.996	7.1
C116	1.88	1.00	11.46	0.153	0.623	4.5	S116	1.96	0.98	13.82	0.153	0.590	4.2
C117	2.39	0.18	11.64	0.079	1.220	8.8	S117	2.09	0.20	15.65	0.078	1.311	9.4
C118	2.48	0.63	11.48	0.089	1.039	7.5	S118	2.36	0.62	13.50	0.083	1.067	7.7
C119	2.45	1.02	13.36	0.153	0.727	5.2	S119	2.19	1.04	15.73	0.153	0.672	4.8

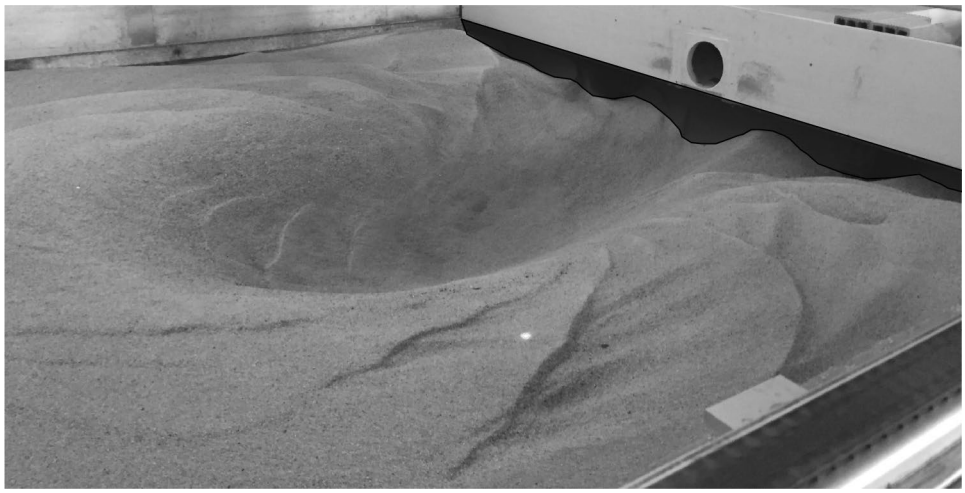

Fig. 2 Final state of the scour hole for the test with the maximum local scour depth, $d_{s,max}/d \approx 2.5$ (test *C004*). Undermining transversal area for the embankment, A_u, appears shadded

tests defined by an equal number of combinations of $Y_u/d = [0.50;1.25;2.00;2.50] \times Y_t/d = [0.15;0.60;1.00]$ were performed. Note that since flow rate is not forced by impinging, only the cases where $Y_u/d > Y_t/d$ make sense. An uniform perforated plate was employed to uniformly block the inlet when needed. On the other hand, culvert wing walls with a floor slab at the outlet were built in methacrylate with both horizontal and vertical angles of 45°.

Previous to the tests, we calibrated both the water flow rate and the tailgate level downstream to obtain the required headwater and tailwater levels with a specific configuration. The flow rate was controlled by an electromagnetic flow meter (± 0.01 l/s) installed in the hydraulic circuit, while depths were measured with a standard measuring device-point gauge (± 0.1 mm). Once these parameters had been adjusted, the bottom was levelled adjacent to the elevation of the culvert invert and the sediment was saturated with a low flow rate before starting. Then, the desired flow rate was gradually entered and scour was immediately initiated. The duration of each experiment was 9 h, taking into account the fact that for all these tests we are interested in the zone located just downstream from the culvert outlets and in this zone the equilibrium time is reduced (Faruque et al. 2006). During each test, the maximum scour depth within the hole was measured with an accuracy of 0.1 mm, using one adapted point gauge at high frequency (up to five measurements in the first hour). Figure 3 shows the evolution of $d_{s,max}$ over time during the total test duration with the adjusted scour depth using an empirical function similar to that proposed by Franzetti et al. (1982), which reads

$$\frac{d_{s,max}}{d_{s,max}^{\infty}} = 1 - \exp\left(-c_1 t^{c_2}\right), \tag{5}$$

where $d_{s,max}^{\infty}$ is the equilibrium scour depth obtained by extrapolating to infinite time the measured scour depths with $c_1, c_2 > 0$ being constants. Although this expression was developed for local scour depth at bridge piers, it seems to reproduce the time evolution of scour depth quite well. In general, the largest scour depth takes place with low tailwater depths and high headwater depths, independently of the culvert shape, being more intense for free inlets and non protected outlets. In the following section these results will be analysed in detail.

Additionally, the flow depth (and so the mean velocity) within the culvert were monitored during the whole test using two video cameras at high frequency when no full-flow at the outlet was observed. Every 5 min five pictures (5 fps) were taken to adequately capture possible oscillations of the free surface and a mean filter to these five images was applied to obtain only one picture each time (109 images/experiment). Finally, we obtained intrinsic camera parameters following Bouguet (2008) and extrinsic calibration according to Simarro et al. (2017) before computing the mean water depth at the culvert outlet using all the 109 mean images. Up to 12 points whose location was known were employed to achieve an adequate calibration. This step is crucial in order to accurately measure the water depth at the culvert outlet and, consequently, the densimetric Froude number.

At the end of each experiment, flow to the system was halted and the gate slowly lowered to expose the local scour pattern. The measure of the final scour hole was carried out measuring an array of points (5 cm × 5 cm) by using a laser distance sensor with an accuracy of ± 0.2 mm. Table 2 shows the main characteristic dimensions of the scour hole normalized by the culvert rise, d, as follows:

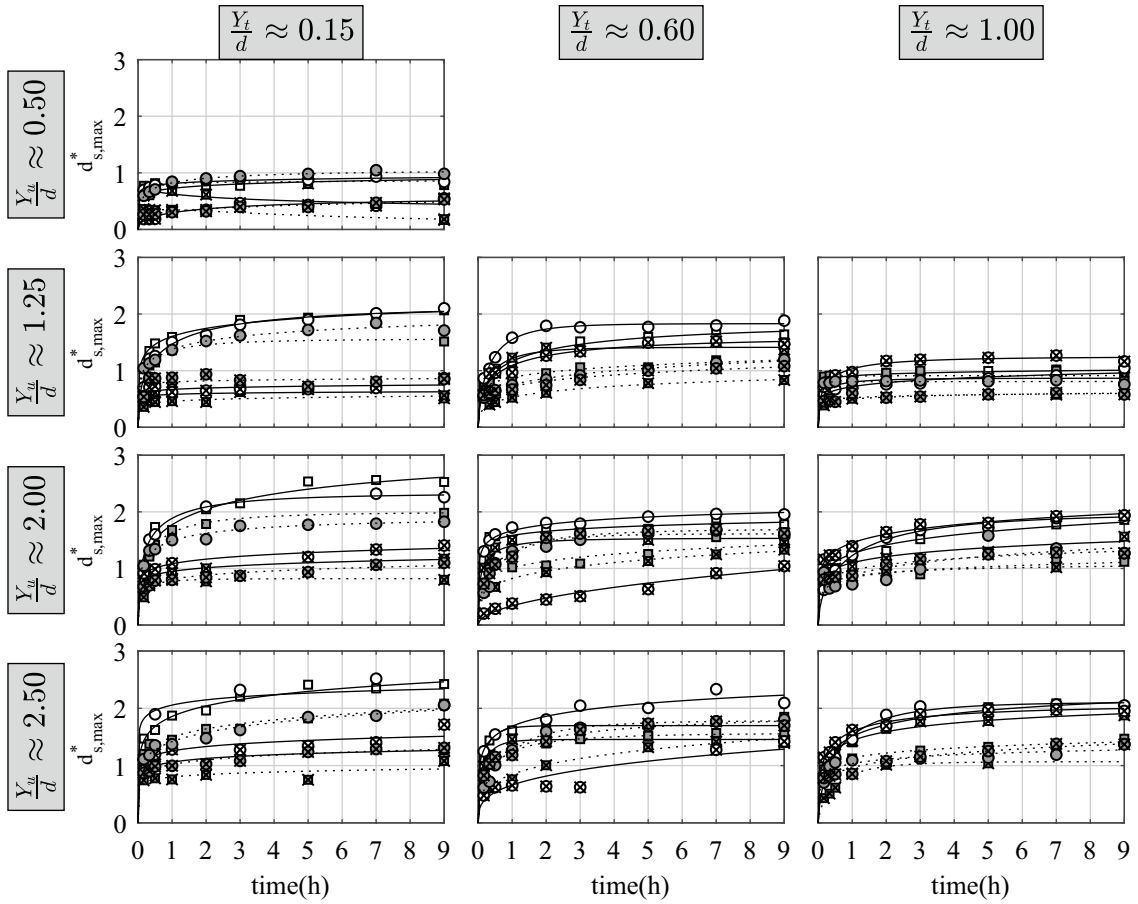

Fig. 3 Maximum scour depth time evolution. Marker shape ≡ culvert shape; free inlet (white marker); blocked inlet (gray marker); free outlet (not crossed out); wing walled outlet (crossed out). The lines represent the adjusted scour depth time evolution, using solid lines for non blocked inlets and dotted lines for blocked inlets

$$L_s^* \equiv \frac{L_s}{d}, \quad W^* \equiv \frac{W}{d}, \quad d_{s,max}^* \equiv \frac{d_{s,max}}{d},$$
$$L_{s,max}^* \equiv \frac{L_{s,max}}{d},$$
$$d_{s,u}^* \equiv \frac{d_{s,u}}{d}, \quad L_{s,u}^* \equiv \frac{L_{s,u}}{d}, \quad A_u^* \equiv \frac{A_u}{d^2}.$$

Above, $d_{s,u}$ is the maximum scour depth within the undermining area, A_u, located just at the culvert outlet and $L_{s,u}$ is the length parallel to the embankment (normal to the culvert axis) affected by the embankment undermining. The complete record of the bottom can be found at https://data.mendeley.com/datasets/pfsdjxf6pb/draft?a=11ca79cc-ad67-41b9-9a32-416abf892c49.

Results and discussion

A summary of the input variables and flow characteristics, including the computing depth at the culvert outlet using video image technique, Y_0, for all the tests is presented in Table 1. As shown, densimetric Froude number takes values up to 17.3, although in the majority of the tests, its value is below 10, i.e., the range within which the densimetric Froude number shows the most influence on the scour. In addition, minimum pipe Reynolds number takes place for the test S103, but even in this case $Re = 6.5 \times 10^4 > 5 \times 10^4$, i.e., scale effects can be neglected.

Table 2 Scour hole dimensions for all the tests

Circular shape ○								Square shape □							
Test	Plant		Longitudinal		Undermining			Test	Plant		Longitudinal		Undermining		
	L_s^*	W^*	$d_{s,max}^*$	$L_{s,max}^*$	$d_{s,u}^*$	$L_{s,u}^*$	A_u^*		L_s^*	W^*	$d_{s,max}^*$	$L_{s,max}^*$	$d_{s,u}^*$	$L_{s,u}^*$	A_u^*
Without wing walls at outlet and non-blocked inlet (0% blockage)															
C000	4.0	4.4	0.9	1.4	0.6	3.9	0.8	S000	17.6	1.0	1.0	17.2	0.4	5.8	0.7
C001	8.9	8.8	2.1	3.2	1.2	13.1	6.1	S001	14.2	13.6	2.1	5.2	1.5	16.4	9.6
C002	11.7	8.2	1.6	4.5	0.7	4.6	1.6	S002	13.5	7.9	1.9	5.9	0.9	12.5	3.5
C003	11.7	4.1	0.9	3.9	0.6	3.9	1.0	S003	12.2	4.4	1.0	4.5	0.7	4.6	1.4
C004	14.4	16.4	2.5	5.6	1.6	16.4	10.9	S004	18.0	16.1	2.3	3.2	1.8	16.1	15.9
C005	18.2	8.8	1.8	4.5	1.2	16.4	9.6	S005	15.4	8.3	2.0	6.3	1.6	16.4	14.7
C006	15.2	8.5	1.9	5.6	0.7	5.2	1.6	S006	19.3	8.3	1.9	7.3	0.6	3.9	1.1
C007	16.9	16.4	2.4	4.5	1.6	16.4	13.7	S007	17.9	16.4	2.1	5.6	1.5	16.4	10.0
C008	19.7	6.9	1.9	4.9	1.2	16.4	9.4	S008	20.9	12.0	2.1	4.5	1.6	16.1	12.8
C009	16.6	9.2	2.0	5.9	0.6	9.2	1.6	S009	18.6	8.6	2.1	5.2	0.6	16.4	3.2
With wing walls at outlet and non-blocked inlet (0% blockage)															
C010	4.4	1.1	0.2	0.3	0.2	5.2	0.8	S010	10.2	6.1	0.5	1.4	0.3	5.9	3.1
C011	12.1	6.7	0.5	1.0	0.5	9.8	5.1	S011	10.7	6.8	0.9	0.5	0.7	16.4	9.0
C012	13.8	5.9	1.4	5.6	0.3	2.6	0.0	S012	18.3	7.8	1.5	4.5	0.6	11.1	1.1
C013	11.4	4.3	0.9	5.2	0.2	3.9	0.2	S013	14.2	4.4	1.2	5.9	0.3	4.6	0.0
C014	20.1	8.4	1.2	1.4	0.7	16.4	6.2	S014	20.9	16.4	1.4	1.4	0.9	16.4	7.8
C015	20.5	6.3	1.5	5.2	0.5	5.2	0.6	S015	1.9	6.8	1.0	0.5	0.8	16.4	13.0
C016	17.5	6.3	1.6	8.2	0.2	4.6	0.1	S016	20.0	7.2	1.9	7.3	0.5	4.6	0.1
C017	20.6	16.4	1.2	8.1	0.7	9.8	5.4	S017	20.9	16.4	1.7	1.4	1.1	16.4	8.6
C018	20.9	6.2	1.4	3.9	0.7	10.5	1.3	S018	17.0	13.7	1.4	1.4	0.9	16.1	12.0
C019	19.5	7.0	1.9	7.6	0.3	3.9	0.1	S019	20.9	7.6	2.0	5.2	0.8	16.4	1.2
Without wing walls at outlet and partially blocked inlet (50% blockage)															
C100	2.8	3.9	0.8	0.7	0.8	4.6	1.4	S100	9.1	5.1	1.0	1.7	0.7	4.6	1.1
C101	6.6	12.8	1.5	0.9	1.4	13.1	7.7	S101	12.3	9.6	1.7	4.2	1.2	13.1	7.2
C102	12.9	4.6	1.2	3.5	0.6	3.9	0.9	S102	16.6	5.1	1.2	5.9	0.6	3.9	1.1
C103	6.7	4.1	0.8	1.4	0.6	3.9	0.9	S103	9.3	3.8	0.8	1.0	0.6	3.9	1.2
C104	12.0	16.4	2.0	3.2	1.3	15.7	8.4	S104	16.0	16.4	1.8	6.3	1.4	16.4	10.6
C105	14.9	6.3	1.4	3.8	0.9	11.8	4.1	S105	20.9	16.4	1.6	4.2	0.6	16.4	2.5
C106	12.1	4.9	1.1	4.2	0.6	3.9	1.0	S106	14.8	4.9	1.3	3.2	0.4	3.9	1.0
C107	13.3	9.5	2.1	3.9	1.5	15.7	8.3	S107	17.9	16.4	2.1	5.6	1.5	16.4	10.0
C108	14.5	11.4	1.6	3.8	0.8	16.4	3.3	S108	17.6	9.2	1.8	3.9	0.7	11.8	2.3
C109	9.6	5.1	1.3	5.6	0.5	3.3	0.8	S109	17.2	5.7	1.4	7.6	0.7	3.9	1.0
With wing walls at outlet and partially blocked inlet (50% blockage)															
C110	3.3	3.0	0.2	2.1	0.1	3.9	0.0	S110	5.1	4.3	0.4	2.8	0.2	4.6	0.5
C111	11.5	5.1	0.5	1.4	0.3	9.2	2.2	S111	19.0	11.8	0.8	1.1	0.8	16.4	7.4
C112	13.9	3.6	0.8	6.6	0.2	3.9	0.0	S112	16.9	4.5	1.1	5.6	0.4	6.6	1.0
C113	6.9	3.6	0.5	4.2	0.1	1.3	0.0	S113	10.7	3.3	0.6	4.5	0.3	5.9	0.6
C114	15.9	10.5	0.8	2.1	0.5	16.4	5.9	S114	20.9	16.4	1.0	1.8	0.8	16.4	8.8
C115	18.6	6.3	1.3	5.2	0.4	2.0	0.2	S115	20.9	7.2	1.6	4.9	0.6	15.7	1.5
C116	13.9	4.3	0.9	5.4	0.1	0.1	0.0	S116	16.6	5.0	1.3	7.3	0.5	10.5	1.5
C117	13.5	8.5	1.0	1.4	0.6	9.2	3.5	S117	20.9	16.4	1.3	1.4	0.8	16.4	5.9
C118	19.1	6.8	1.4	4.9	0.3	2.0	0.2	S118	20.9	8.9	1.7	4.9	0.6	16.4	1.8
C119	17.4	4.5	1.2	8.4	0.2	4.6	0.2	S119	17.2	16.4	1.4	7.3	0.6	16.4	2.7

In order to analyse the main factors affecting the most important dimensions, an analysis of variance (ANOVA) was carried out with the results shown in Tables 1 and 2. The use of ANOVA models provides the user a statistically based technique capable of producing meaningful models on the importance of the factors studied

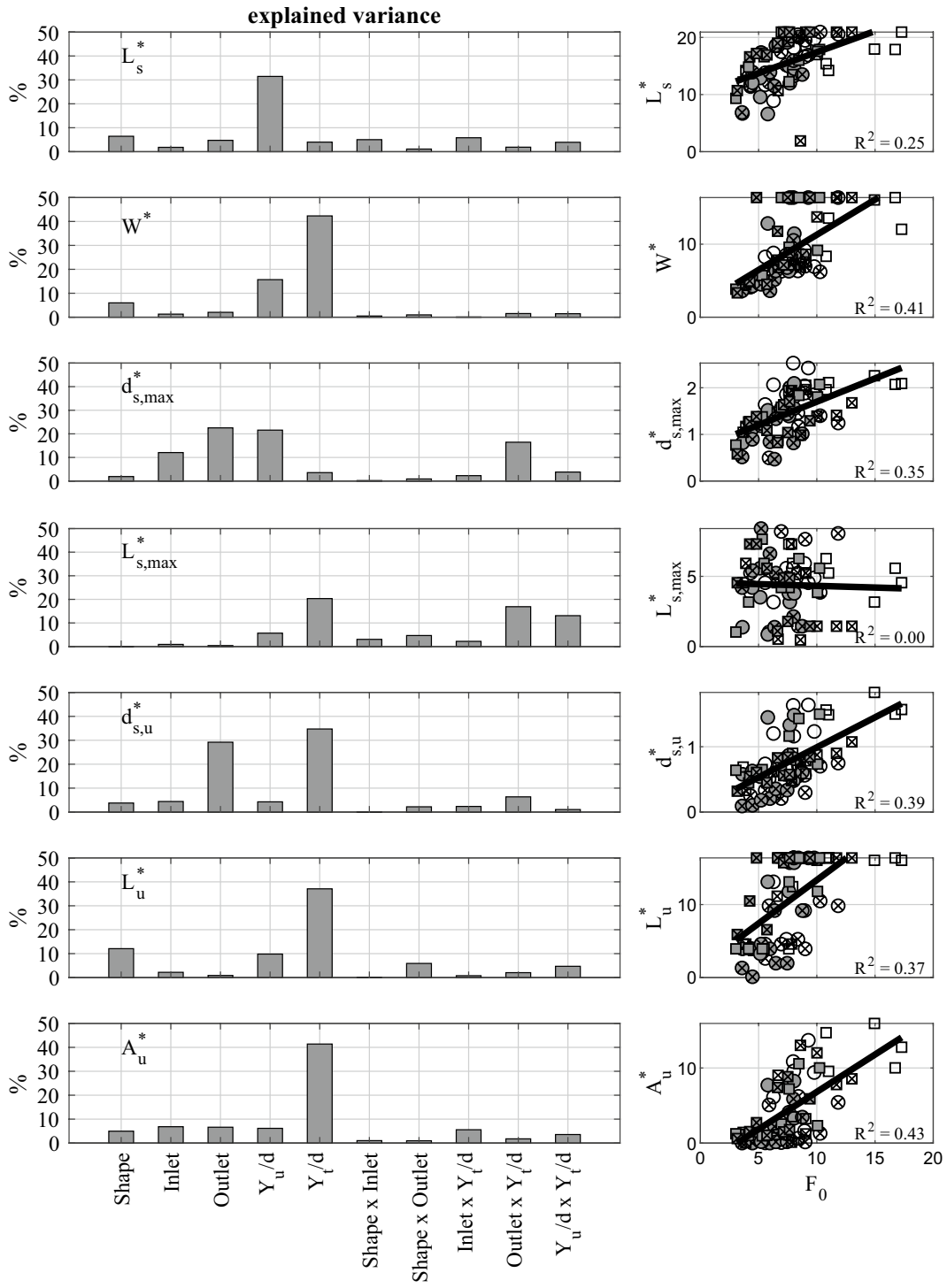

Fig. 4 ANOVA analysis for the % of variance explained (left) and correlation between densimetric Froude number and geometric variables defining local scour (right). Marker shape ≡ culvert shape; free inlet (white marker); blocked inlet (grey marker); free outlet (not crossed out); wing walled outlet (crossed out)

in the experiment (Cox and Reid 2000). Apart from this, ANOVA allows possible factors interactions within the data set that may have a bearing on the scour hole dimensions previously defined. Figure 4 shows the percentage of the total variance explained by the independent variables and their interactions whose p values are larger or equal to 0.01 (selected significance). Within the factors affecting the variance are considered the three ones discussed in

"Framework for analysis", plus the particular conditions of culvert geometry and blockage. For more of these factors a limited number of values/conditions have been experimented, and the ANOVA have been performed both in one and two ways ANOVA, to study first-order interactions. In the case of densimetric Froude number, because it has been evaluated in a broad range of values, the regression analysis has been performed. The main conclusions which could be extracted from the Figure are the following: (1) the hole length, L_s^*, is mainly influenced by the headwater depth and, to a lesser extent, by the culvert shape; (2) the three parameters dominating the hole width, W_s^*, are, in order of importance, the tailwater depth, the headwater depth and the culvert shape; (3) with respect to the maximum local scour within the hole, $d_{s,max}^*$, the outlet configuration, its interaction with the tailwater depth, the headwater depth and the inlet configuration are the most representative parameters, while the location of this maximum local scour, $L_{s,max}^*$, is dominated by the tailwater depth and secondarily by the interaction between this and the outlet configuration and the available energy (interaction between headwater and tailwater depths.); (4) the embankment undermining is mainly dominated by the tailwater depth since the three dimensions, $d_{s,u}^*$, L_u^* and A_u^* heavily depend on it. The rest of the variables affecting the embankment undermining are, in order of importance, the outlet configuration (influencing on $d_{s,u}^*$), the barrel shape and the headwater depth (both with significant influence on L_u^*). Additionally, Fig. 4 shows the correlation between the densimetric Froude number and the scour hole dimensions (right). The densimetric Froude number is well correlated ($R^2 > 0.25$ implies that more than a quarter of the observed variation can be explained by the Froude number) with all the studied dimensions (the length increases with F_0) except with $L_{s,max}^*$. In addition, note that in all cases, tests with blocked inlets follow the same tendency as tests with free inlets, which could indicate that the densimetric Froude number, F_0, is not only properly absorbing the effects of sediment size but also the effects of blockage at the inlet, so an accurate prediction of water depth at the culvert outlet together with the flow rate estimation is necessary. In contrast, the presence or not of wing walls at the outlet seems to create a larger dispersion of the data when correlated with F_0. This result is consequent to the fact that the densimetric Froude number is affected by the flow inside the culvert but not with the outlet configuration (inlet control in most of the cases).

Therefore, several factors are affecting scour hole geometry. The four most important are the outlet water depth, the upstream water depth, the outlet conditions, plus the densimetric Froude number. This is in agreement with Eq. (4) (no factor may be neglected), but the model may be particularized with every outlet conditions.

Scour hole plant: length and width

As mentioned above, the main factors influencing the scour hole plant are primarily both the headwater and tailwater depths, and secondarily the culvert shape, with the influence of the rest of the parameters and their interactions being less than 5% in terms of the total explained variance. For simplicity reasons, Fig. 5 shows the plant view of the scour hole only for the tests with free inlets since they generate the most extensive holes (contour line at the undisturbed original bed elevation). As shown, the widest scour holes take place for low tailwater depths (left column in the figure) for any outlet configuration and culvert shape, scouring the whole width of the receiving channel for all the tests except for the one with the lowest headwater depth. As tailwater level increases (center and right columns), the scour hole becomes narrower with the mean reduction of the scour hole width being up to 14% and 35% for medium and high tailwater, respectively, with respect to the lowest tailwater, and only with square culverts (grey lines) is the whole width of the channel eroded, mainly with medium and high headwater levels. In summary, the scour hole width becomes larger when the tailwater depth decreases or/and when the headwater level increases. In any case, the scour hole is wider and longer for square culverts than for the circular ones (the means values and standard deviations are $W^{\text{square}}/W^{\text{circular}} = 1.35 \pm 0.52$ and $L_s^{\text{square}}/L_s^{\text{circular}} = 1.32 \pm 0.44$, respectively) which could indicate that the flow has better transversal distribution at the outlet for square shapes than for circular ones, as noted before by Chen (1970) and Abt et al. (1987), creating a preferential flow direction parallel to the barrel axis in this case. With respect to the scour hole length, L_s, it seems clear that it increases as headwater depth grows for all analysed tests. From Fig. 5, the effect of wing walls at the outlet is noticeable since, in the vast majority of the tests, the presence of protected outlets (indicated with crosses in the figure) creates longer scour holes but it does not significantly affect the hole width ($W^{\text{wing-walled}}/W^{\text{non-wing-walled}} = 1.01 \pm 0.36$ and $L_s^{\text{wing-walled}}/L_s^{\text{non-wing-walled}} = 1.17 \pm 0.20$). Because the wing walls have a floor slab, it can contribute to redirecting the flow from the bottom to the free surface. Without wing walls, the vertical component of the flow at the culvert outlet directly impacts the bed, while with the floor slab it is deviated by the fixed bottom reducing the vertical velocity component of the jet. Since the discharge is smaller (with same headwater and tailwater depths) for blocked inlets, the hole extension is shorter too ($W^{\text{blocked}}/W^{\text{non-blocked}} = 0.79 \pm 0.24$ and $L_s^{\text{blocked}}/L_s^{\text{non-blocked}} = 0.89 \pm 0.18$).

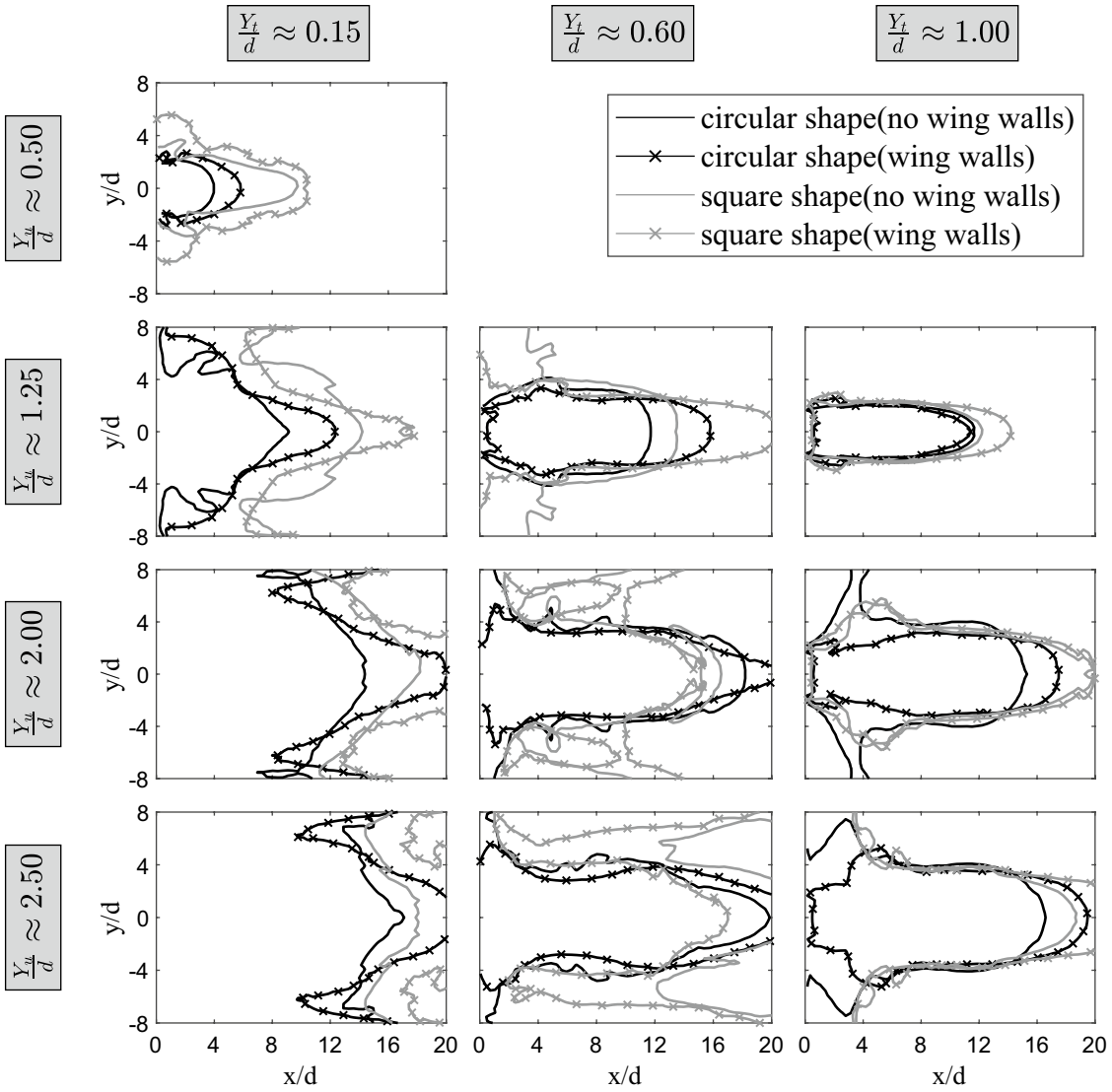

Fig. 5 Plant view of local scour hole for non blocked inlets. Line colour refers to the culvert shape (black for circular culverts and grey for square culverts). The presence of wing walls is marked with crosses

Scour hole profile: maximum scour depth and its location

The maximum scour depth, $d_{s,max}$, is perhaps the most studied scour hole characteristic dimension over the past few decades. Most of the previous mentioned in the "*Introduction"* section studies have noted the influence of multiple variables among which the culvert shape and densimetric Froude number stand out, but none of them highlights the influence of wing walls and a floor slab at the outlet even though, according to the previous analysis of variance, it is the most relevant variable. Figure 6 shows the longitudinal scour profile at the channel centreline and the location of $d_{s,max}$ for all the performed tests. For free outlets, the maximum values of $d_{s,max}$ for all values of Y_u/d take place with low tailwater depths (dotted lines), being smaller for the square barrel compared with the circular one even when the discharge is higher in that case. This effect can be explained for the flow characteristics at the outlet. For the circular shape, the flow concentrates at the centreline of the barrel and produces an important impact on the bottom just downstream. By contrast, the square shape produces a better flow distribution along the transversal direction, as noted before. Note that this shape effect dissipates for medium (dotdash lines) and high (solid lines) tailwater depths. In these cases, a water mattress exists downstream from the culvert outlet that mitigates the impact of the jet and minimizes the importance of the flow distribution at the outlet in the maximum local scour. When wing-walled outlets are analysed, maximum scour depth for low

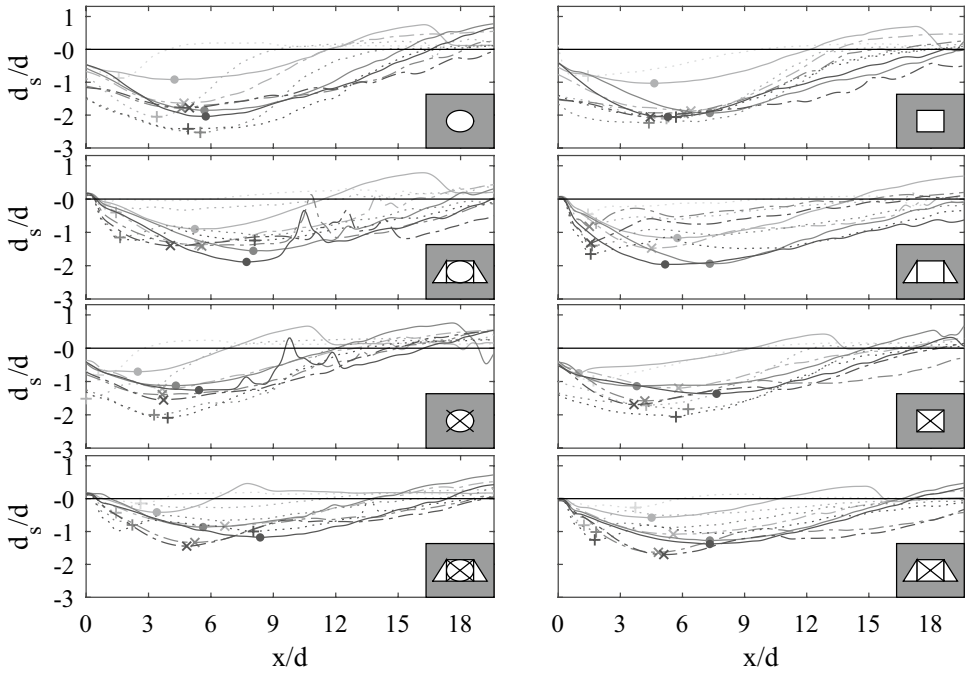

Fig. 6 Longitudinal profile of local scour, d_s/d, through the centreline. Line colour refers to the headwater depth (lighter colours for low headwater depth and darker ones for higher values) and line type refers to the tailwater depth (dotted lines for $Y_t/d \approx 0.15$, dotdash lines for $Y_t/d \approx 0.60$ and solid lines for $Y_t/d \approx 1.0$). Pluses, crosses and dots locate the position of $d_{s,max}$ for low, medium and high tailwater depths, respectively

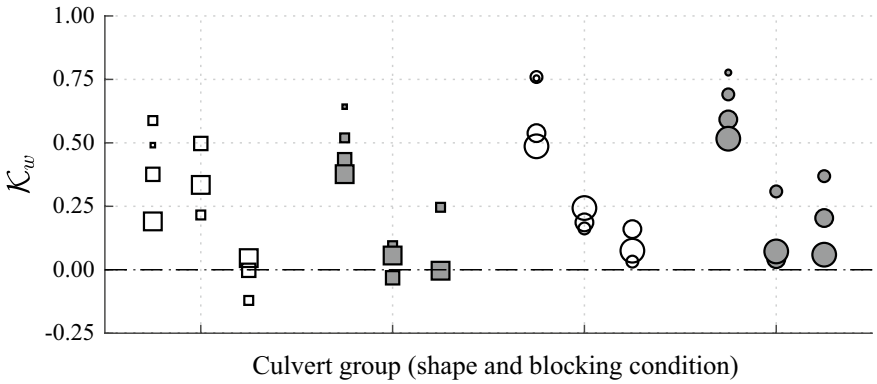

Fig. 7 Wing walls coefficient, $\mathcal{K}_w$. Marker shape ≡ culvert shape; free inlet (white marker); blocked inlet (grey marker); the sizes are proportional to the four headwater depths. For each group, low tailwater is on the left, medium tailwater is in the middle and high tailwater is on the right

tailwater depths is strongly diminished while for medium and high values of Y_t, the maximum local scour is very similar with and without wing walls. For medium and high tailwater depths the wing walls are less effective. Figure 7 shows the value of the wing walls coefficient, $\mathcal{K}_w$, which measures the reduction of maximum scour depth due to the presence of wing walls, defined as

$$\mathcal{K}_w \equiv \frac{d^{\diamondsuit}_{s,max} - d^{\boxtimes\diamondsuit}_{s,max}}{d^{\diamondsuit}_{s,max}}. \quad (6)$$

where $d^{\diamondsuit}_{s,max}$ and $d^{\boxtimes\diamondsuit}_{s,max}$ are the maximum scour depths for free and wing walled outlets, respectively, under the same conditions of headwater and tailwater depth, blocked inlet percentage and culvert shape. In most of the tests, the influence of wing walls at the outlet is quite positive, reducing the maximum scour depth even more than 75% for three tests with low tailwater, low headwater depths and circular shape in comparison to the same test with free outlet (the mean reduction for low tailwater depth is close to 55%). This effect is less significant for medium and high tailwater depths, with a mean reduction of 18% and 9%, respectively.

The second most influencing parameter on maximum scour depth, Y_u, is closely related to F_0, as shown in Table 1. Figure 8 shows the value of $d_{s,max}$ normalized with the culvert rise, d, against the densimetric Froude number, F_0, since, as pointed out before by Lim (1995), $d_{s,max}$ increases its value with F_0 into the range where $F_0 \leq 10$ and for any possible configuration, this behaviour is observed for the presented tests. Note that with a free outlet without wing walls (top panels), non-blocked and partially blocked culverts have a similar performance for any barrel shape which indicates that the densimetric Froude number, F_0,

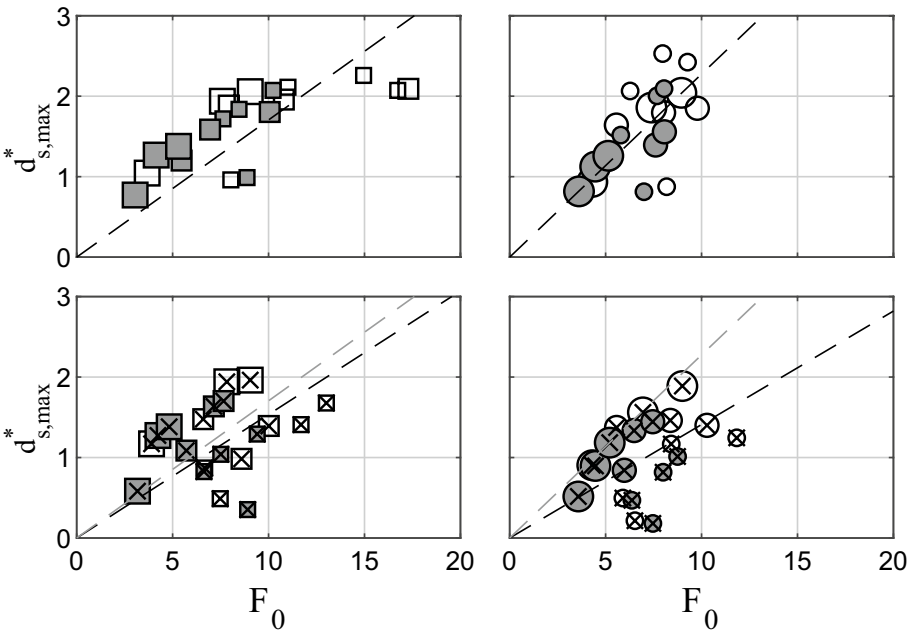

Fig. 8 Maximum local scour against densimetric Froude number. Marker shape ≡ culvert shape; free inlet (white marker); blocked inlet (grey marker); free outlet (not crossed out); wing walled outlet (crossed out); the three different marker sizes refer to the three tailwater depths

is absorbing the effects of the blockage at the inlet. Correspondingly, F_0 retains information of both the flow rate and the flow depth at the culvert outlet, which is quite influenced by the inlet condition. In addition to the aforementioned information about wing walls effects, it seems clear for both analysed shapes that the presence of wing walls at the outlet produces a larger dispersion of the data, with the dependence of maximum scour depth with F_0 being less evident (bottom panels in the Fig. 8). Since wing walls are more effective when low tailwater depths take place, in the bottom panels of Fig. 8 these values deviate from those with medium and high tailwater depths. Again, the fact that the reduction of scour depth is greater for circular shapes than for square shapes is evident when comparing the slope of the fitted lines for both free outlets (grey lines in Fig. 8) and wing-walled outlets.

With regard to the inlet blocking effect, it is clear from Fig. 6 that in all cases $d_{s,max}$ decreases for blocked inlet with respect to the free inlet condition, with this reduction being clearer for medium and high tailwater depths and negligible for low values of Y_t (even when the flow discharge is considerably smaller for blocked inlets). This effect has significant implications since for a fixed flow discharge the blockage of the inlet increases the necessary headwater depth and the expected local scour, as shown, is related with the headwater depth, Y_u, instead of the flow discharge, Q.

Regarding the location of $d_{s,max}$, even when quite large, if it is located far from the outlet and the embankment is not affected, there is no risk of instability. By contrast, if the location of the maximum scour depth is close enough to the embankment, and this value being smaller, this could induce the scouring of the culvert and the embankment failure. In this sense, the distance between the culvert outlet and the point where the maximum scour depth is located, $L_{s,max}$, plays an important role and, for the tests, a value of $L_{s,max} \approx (0.294 \pm 0.165)L_s$ has been found, with L_s being the longitudinal length of the scour hole. This value is quite close to that encountered by Fletcher and Grace (1972). Culvert rise can be used as a characteristic variable $L_{s,max} \approx (4.27 \pm 2.62)d$, although a general trend, the lower the tailwater depth, the shorter the distance from the maximum scour depth to the culvert outlet. This same trend is also found with headwater depths, except for submerged outlets for which the scour depth distance diminishes with the headwater depth. For low and medium tailwater depths, maximum scour depth location depends heavily on the available energy at the culvert since, as noted before, the downstream water mattress is not high enough to deflect the jet closer to the outlet. Nonetheless, for high tailwater depths, i.e., submerged outlets, the jet direction is modified by the water mattress and this is redirected near the bottom, producing a greater scour near the culvert outlet and, therefore, increasing the risk of undermining for the structure. For wing walled outlets, the lowest tailwater depths show a different behavior than the higher ones, and in all cases, they produce the nearest scour to the culvert outlet.

Embankment undermining

The undermining of the embankment is perhaps the most important variable affecting the whole stability of the infrastructure; however, to the author's knowledge, there are no studies about the influence of the considered independent variables on it. Since a cantilevered embankment

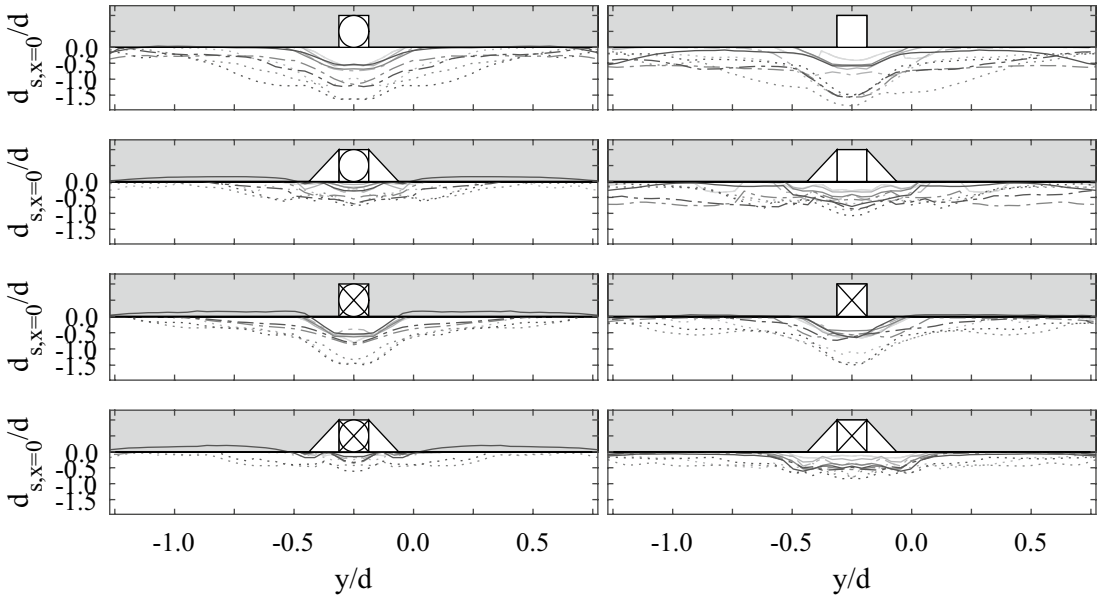

Fig. 9 Transversal profile of local scour, d_s through the embankment line. Line colour refers to the headwater depth (lighter colours for low headwater depth and darker ones for higher values) and line type refers to the tailwater depth (dotted lines for $Y_t/d \approx 0.15$, dotdash lines for $Y_t/d \approx 0.60$ and solid lines for $Y_t/d \approx 1.0$)

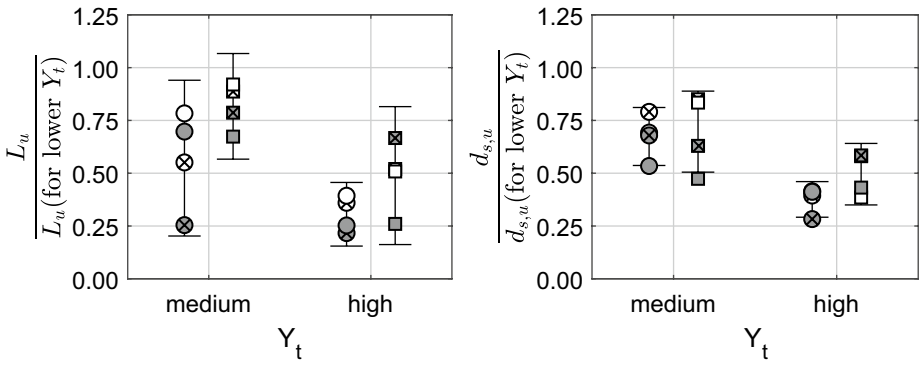

Fig. 10 Mean and standard deviation (vertical lines) for the ratio of diminishing undermining with the tailwater depth (analysing all the tests). Marker shape ≡ culvert shape; free inlet (white marker); blocked inlet (grey marker); free outlet (not crossed out); wing walled outlet (crossed out)

configuration has been chosen in this study (see Fig. 1), the undermining of it can be measured as shown in Fig. 9.

As shown in Fig. 4, tailwater depth seems to be the most relevant variable affecting the embankment undermining. Figure 10 shows the relationships between $d_{s,u}$ and L_u for medium and high tailwater depths when compared to those for tests with minimum tailwater depths. The mean value for the ratio of L_u for medium tailwater depths is 0.57 for circular culverts and 0.81 for square culverts, with these values being 0.3 and 0.49, respectively, for the highest tailwater depths. As noted before, the water mattress downstream from the culvert reduces the local scour, being more effective for circular barrels than for square ones. Similar values are found for $d_{s,u}$ but with less dispersion in the data since the standard deviation is smaller in this case. These results imply that, for the highest tailwater depths, the diminishing of the embankment undermining can reach values of up to 70% when compared with the lowest analyzed tailwater depths for any possible combination of inlet-outlet configuration.

Another important variable when analysing $d_{s,u}$, as detected by the ANOVA analysis, is the presence or not of wing walls at the outlet. Figure 11 shows the value of the wing walls coefficient for the variable $d_{s,u}$, named as $\mathcal{K}_w^u$, which measures the reduction of maximum undermining depth due to the presence of wing walls, defined as

$$\mathcal{K}_w^u \equiv \frac{d_{s,u}^{\diamondsuit} - d_{s,u}^{\diamondsuit\!\!\!\!\diamondsuit}}{d_{s,u}^{\diamondsuit}} \tag{7}$$

where $d_{s,u}^{\diamondsuit}$ and $d_{s,u}^{\diamondsuit\!\!\!\!\diamondsuit}$ are the maximum undermining depth for free and wing walled outlets, respectively, under the same

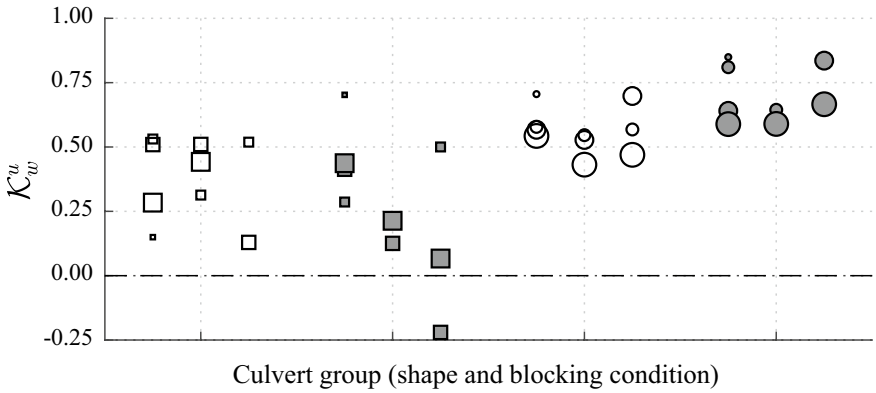

Fig. 11 Wing walls coefficient, $\mathcal{K}_w^u$ for maximum undermining depth. Marker shape ≡ culvert shape; free inlet (white marker); blocked inlet (grey marker); the sizes are proportional to the four headwater depths. For each group, low tailwater is on the left, medium tailwater is in the middle and high tailwater is on the right

conditions of headwater and tailwater depth, blockage inlet percentage and culvert shape.

As for the maximum scour depth within the scour hole, in most of the tests the influence of wing walls at the outlet is quite positive, reducing the maximum undermining depth as well. However, the reduction in this case is less dependent on the tailwater depth than for $d_{s,max}$. In contrast, $\mathcal{K}_s^u$, strongly depends on the culvert shape, with a mean reduction of 63% for circular barrels and 29% for square barrels. Note that the culvert shape does not show any influence on the undermining depth when it is independently analysed ($d_{s,u}^{square}/d_{s,u}^{circular} \approx 1.01 \pm 0.2$), but it does influence the affected length since $L_{s,u}$ is larger for square culverts than for the equivalent test with a circular barrel. The mean value of the ratio $L_{s,u}^{square}/L_{s,u}^{circular}$ is 1.18 for non-protected outlets while when wing walls are used the mean value is 2.76.

Concluding remarks

In this study, 80 experiments were performed to find the characteristic variables influencing the local scour at the culvert outlets (plant and profile of the scour hole and embankment undermining), mainly the headwater depth, the tailwater depth, the inlet condition, the outlet configuration and the culvert shape. The special set up of the experiments allows the direct measure of the embankment undermining which could increase the embankment failure probability. The densimetric Froude number has proved to be capable of capturing the influence of the inlet obstruction as well as the size of the sediment, but not the influence of the wing walls at the outlet. The culvert shape influences the scour hole length and width, with these lengths being larger for square culverts than for circular ones. However, the maximum scour depth within the scour hole is smaller for square culverts, especially for low tailwater depths. This condition of tailwater depth produces scour holes which are the widest, deepest and closest to the culvert outlet and consequently, the widest and deepest embankment undermining. As the tailwater depth increases the scour holes become narrower and shallower, with the maximum scour depth being located further from the embankment and reducing the scoured area below it. Additionally, the use of wing walls with a floor slab at the culvert outlet has significant effects on all of these dimensions. First, the wing walls produce a flow redistribution both in plant and profile, modifying the flow pattern and the scour hole size (the length increases and the scour depth strongly diminishes for low tailwater depths). This effect is more significant for circular barrels than for square barrels, which can be explained by the different flow pattern inside the barrel for each barrel shape. The embankment undermining is also reduced by the presence of wing walls, again more noticeable for circular culverts. Regarding the inlet blockage, even when the flow rate is smaller than for free inlets and it produces smaller scour holes, the embankment undermining is similar in both cases for the same headwater depths. Nevertheless, with the same flow rate the required headwater depth increases for blocked inlets, which generates larger scour holes and embankment undermining. This work lays the foundations for future research on the quantitative effects of the main factors affecting embankment undermining and, therefore, to obtain new empirical relationships to quantify the risk of the structures.

Acknowledgements This work was funded by the project BIA2014-53302-R, Programa Estatal de Investigación, Desarrollo e Innovación Orientada a los Retos de la Sociedad. Ministerio de Economía y Competitividad. Gobierno de Espaa.

References

Abida H, Townsend R (1991) Local scour downstream of box-culvert outlets. J Irrig Drain Eng 117(3):425–440

Abt SR, Kloberdanz RL, Mendoza C (1984) Unified culvert scour determination. J Hydraul Eng 110(10):1475–1479

Abt SR et al (1987) Influence of culvert shape on outlet scour. J Hydraul Eng 113(3):393–400
Abt SR, Thompson P, Lewis T (1996) Enhancement of the culvert outlet scour estimation equations. Transp Res Rec J Transp Res Board 1523:178–185
Ade F, Rajaratman N (1998) Generalized study of erosion by circular horizontal turbulent jets. J Hydraul Res 36(4):613–636
Ali KHM, Lim SY (1986) Local scour caused by submerged wall jets. Proc Inst Civ Eng 81(4):607–645
Azamathulla HM, Haque AAM (2012) Prediction of scour depth at culvert outlets using gene-expression programming. Int J Innov Comput Inf Control 8:5045–5054
Balachandar R, Reddy H (2013) Scour caused by wall jets. In: Manning AJ (ed) Earth and planetary sciences - sediment transport processes and their modelling applications, Chap 8, pp 177–210
Bohan J (1970) Erosion and riprap requirements at culvert and storm-drain outlets. US Army Engineer Waterways Experiment Station, Vicksburg, Mississippi
Boroomand MR, Neyshabouri SAAS, Aghajanloo K (2007) Numerical simulation of sediment transport and scouring by an offset jet. Can J Civ Eng 34(10):1267–1275
Bouguet JY (2008) Camera calibration toolbox for Matlab. Retrieved from http://www.vision.caltech.edu/bouguetj/calib_doc/
Breusers HNC, Raudkivi AJ (1991) Scouring: hydraulic structures design manual series. CRC Press, Boca Raton
Chen YH (1970) Scour at outlets of box culverts. Thesis (Masters). Colorado State University
Cox DR, Reid N (2000) The theory of the design of experiments. Monographs on atatistics and applied probability. Chapman and Hall/CRC, Boca Raton
Day R, Liriano SL, White WR (2001) Effect of tailwater depth and model scale on scour at culvert outlets. In: Proceedings of the ICE—Water and Maritime Engineering
Donnell CA, Abt SR (1983) Culvert shape effects of localized scou. Hydraulic Engineering Publication, Colorado State University, CER82-83CADSRA42
Emami S, Schleiss AJ (2006) Design of erosion protection at diversion tunnel outlets with concrete prisms. Can J Civ Eng 33(1):81–92
Faruque MAA, Sarathi P, Balachandar R (2006) Clear water local scour by submerged three-dimensional wall jets: effect of tailwater depth. J Hydraul Eng 132(6):575–580
Fletcher BP, Grace JL (1972) Practical guidance for estimating and controlling erosion at culvert outlet. US Army Waterways Experiment Station
Franzetti S, Larcan E, Mingosa P (1982) Influence of tests duration on the evaluation of ultimate scour around circular piers. International conference on the hydraulic modeling of civil engineering structures. BHRA Fluid Engineering, pp 381–396
Heimbecher F, Kaundinya I (2010) Protection of vulnerable infrastructures in a road transport network. In: Transport research Arena Europe. Brussels, pp 1–10
Karim OA, Ali KHM (2000) Prediction of flow patterns in local scour holes caused by turbulent water jets. J Hydraul Res 38(4):279–287
Karki R, Faruque MAA, Balachandar R (2007) Local scour by submerged offset jets. Proc Inst Civ Eng Water Manag 160(3):169–179
Kells JA, Balachandar R, Hagel KP (2001) Effect of grain size on local channel scour below a sluice gate. Can J Civ Eng 28(3):440–451
Lim SY (1995) Scour below unsubmerged full-flowing culvert outlets. Proc Inst Civ Eng Water Mar Energy 112(2):136–149
Liriano S, Day R (2001) Prediction of scour depth at culvert outlets using neural networks. J Hydroinf 3(4):231–238. Original article can be found at: http://www.iwaponline.com/jh/toc.htm Copyright IWA Publishing [Full text of this article is not available in the UHRA]
Melville BW, Lim SY (2014) Scour caused by 2D horizontal jets. J Hydraul Eng 140(2):149–155
Mendoza C, Abt SR, Ruff JF (1983) Headwall influence on scour at culvert outlets. J Hydraul Eng 109(7):1056–1060
Opie TR (1967) Scour at culvert outlets. Thesis (PhD). Colorado State University
Rajaratnam N, Berry B (1977) Erosion by circular turbulent wall jets. J Hydraul Res 15(3):277–289
Ruff JF et al (1982) Scour at culvert outlets in mixed bed materials. US Department of Transportation. Federal Highway Administration
Sarathi P, Faruque MAA, Balachandar R (2008) Influence of tailwater depth, sediment size and densimetric froude number on scour by submerged square wall jets. J Hydraul Res 46(2):158–175
Simarro G et al (2017) Ulises: an open source code for extrinsic calibrations and plan view generations in coastal video monitoring systems. J Coast Res 33(5):1217–1227
Sorourian S (2015) Turbulent flow characteristics at the outlet of partially blocked box culverts. In: E-proceedings of the 36th IAHR World Congress, The Hague, The Netherlands
Sorourian S et al (2014a) Blockage effects on scouring downstream of box culverts under unsteady flow. Aust J Water Res 18(2):180–190
Sorourian S et al. (2014b) Location of the maximum scouring depth at the outlet of partially-blocked and non-blocked box culvert. In: Proceedings of the International Conference on Fluvial Hydraulics, RIVER FLOW, pp 1475–1480
Sui J, Faruque MAA, Balachandar R (2008) Influence of channel width and tailwater depth on local scour caused by square jets. J Hydro Environ Res 2(1):39–45